Published in final edited form as:
Eur J Immunol. 2014 February ; 44(2): 397–408. doi:10.1002/eji.201343587.

Both infection with *Pneumocystis* and virus-like particle exposure prime pulmonary CD11c$^+$ cells, facilitating accelerated immune responses to influenza

Laura E. Richert[1], **Agnieszka Rynda-Apple**[1], **Ann L. Harmsen**[1], **Soo Han**[1], **James A. Wiley**[1], **Trevor Douglas**[2], **Kyle Larson**[1], **Rachelle V. Morton**[1], and **Allen G. Harmsen**[1]

[1]Department of Immunology and Infectious Diseases, Montana State University, Bozeman, Montana, USA.

[2]Department of Chemistry and Biochemistry, Montana State University, Bozeman, USA.

Summary

We show that the intranasal delivery of non-replicative virus-like particles (VLPs), which bear structural, but no antigenic similarities to respiratory pathogens, acted to prime the lungs of mice to facilitate heightened and accelerated primary immune responses to high-dose influenza challenge, thus providing a non-pathogenic model of innate imprinting. These responses corresponded closely to those observed following natural infection with the opportunistic fungus, *Pneumocystis murina*, and were characterized by accelerated antigen processing by dendritic cells (DCs) and alveolar macrophages (AMs), an enhanced influx of cells to the local tracheobronchial lymph node (TBLN), and early upregulation of T cell co-stimulatory/adhesion molecules. CD11c$^+$ cells (DCs and AMs) which had been directly exposed to VLPs or *Pneumocystis* were necessary in facilitating the observed enhanced clearance of influenza virus. Furthermore, the repopulation of the lung by Ly-6C$^+$ myeloid precursors relied on the expression of CCR2, and in the absence of efficient CCR2-mediated trafficking, resistance to influenza afforded by VLP- or *Pneumocystis*-exposure was lost. Thus, immune imprinting 72 hours after VLP-, or 2 weeks after *Pneumocystis*-priming was CCR2-mediated and resulted from the enhanced antigen processing, maturation, and trafficking abilities of DCs and AMs, which caused accelerated influenza-specific primary immune responses, and resulted in superior viral clearance.

Keywords

Innate imprinting; Influenza; Dendritic cell; *Pneumocystis*; CCR2

Introduction

Recent evidence suggests that each antigen/pathogen exposure in the lungs may impact the immunological identity (skewing) and vigor of subsequent unrelated responses, as has been documented for sequential combinations of challenges with many diverse pathogens [1–5]. Pathogen or antigen challenges may thus either augment or dampen future heterologous challenges, depending on the individual's unique history of previous pathogen exposure [6,

Address correspondence to: Dr. Allen G. Harmsen, 960 Technology Blvd., Bozeman, MT 59718. Telephone: (406) 994-7626. Fax: (406) 994-4303. aharmsen@montana.edu.

Supporting Information available online

Conflict of Interest
The authors declare no conflict of interest.

7]. While these responses may be partially governed by cross-reactive T cells [8, 9] or haplotype anomalies [7], heterologous innate immunity also plays an important role in pathogen clearance in a process referred to as innate imprinting [2, 4, 10]. Thus, while we recognize the clinical significance of an individual's immune history, we still do not fully understand many of the underlying cellular mechanisms which govern the phenomenon of innate imprinting. We have recently shown that exposure of the lungs to virus-like particles (VLPs) have effects on the innate resistance of the lungs to subsequent infection, similar to innate imprinting [11]. Here, we elucidate the cellular contributions of innate imprinting by illustrating that the intranasal delivery of either non-replicating VLPs, which bear no antigenic similarities to agents of future challenge, or natural infection (and recovery from) the ubiquitous opportunistic fungi, *Pneumocystis murina* (hereafter referred to as *Pneumocystis*) similarly modulate the pulmonary microenvironment (despite their unrelated immunological identities), facilitating enhanced resistance to a subsequent primary influenza virus challenge.

The VLPs used here are derived from small heat shock protein cage nanoparticles [12–14], which as we have demonstrated in earlier work, can be safely administered into the lung, and do not bioaccumulate with multiple doses [15, 16]. Separately, we have also previously studied the outcome of primary influenza infection in the lungs of mice which have recovered from *Pneumocystis* infection, and found that the influenza viral load is significantly reduced 7 days after infection in the lungs of *Pneumocystis*-exposed mice [1]. We thus demonstrate in the following studies that previous *Pneumocystis*- or VLP-instillation facilitated accelerated influenza virus clearance and enhanced immunity through accelerated dendritic cell (DC)-, as well as alveolar macrophage (AM)-trafficking and antigen processing. For VLP-exposed mice, very early migration of both airway ($CD103^+$), and parenchymal ($CD11b^+$) DCs to the tracheobronchial lymph node (TBLN), as well as the upregulation of T cell co-stimulatory/maturation surface antigens, intracellular adhesion molecule-1 (ICAM-1) and vascular cell adhesion molecule-1 (VCAM-1), appeared to aid in the acceleration of viral clearance and enhanced resistance of the lungs. Additionally, these responses were dependent upon the presence of $CD11c^+$ cells which had been directly exposed to VLPs, as $CD11c^+$ cells which repopulated the lung in the absence of VLPs or *Pneumocystis* (despite previous exposure to either treatment) did not provide protective effects. Ly-$6C^{hi}$ monocytes were also essential to the protection against influenza infection in both *Pneumocystis*- and VLP-primed mice, and in the absence of Ly-$6C^{hi}$ cells in the effector site specifically during VLP- or *Pneumocystis*-priming (in *Ccr2*$^{-/-}$ mice), this protection was lost. Thus, we demonstrate a mechanism of innate imprinting by which a VLP- or *Pneumocystis*-primed lung, lacking any memory cells to agents of subsequent challenge, elicited alternative cellular trafficking and expansion patterns, and thus allowed for viral clearance at an accelerated rate (and potentially enhanced resistance), with less harmful consequence. Importantly, it has been suggested by us [16, 17], and others [18–22] that such harnessing of local mucosal immunity may pose an important clinical approach to the augmentation of pathogen clearance. Given that humans do not exist in a sterile environment, understanding the interplay between pulmonary immune history and subsequent disease processes could provide significant insight in understanding differing levels of susceptibility to infectious diseases of individuals in a population.

Results

Both natural infection with *Pneumocystis*, and the exposure of the lungs to non-replicative VLPs provide protection against morbidity and enhance the clearance of an unrelated pathogen

We analyzed two groups of mice whose lungs were primed via two immunologically disparate scenarios—either infection with 10^7 *Pneumocystis* organisms, or the repeated intranasal (i.n.) administration of VLPs (5 doses), as we have previously described [1, 16]. *Pneumocystis*-infected mice were allowed to recover for two weeks, and VLP- or control DPBS-dosed mice were rested for 72 hours prior to challenge with 1500 pfu A/PR/8/34 (PR8) influenza virus. The timing for each priming scenario was previously determined as the point of peak resistance to subsequent challenge with influenza virus. All mice were weighed daily post-influenza infection, and importantly, we found that both *Pneumocystis*-infected and recovered, and VLP-primed mice were equally protected from influenza-associated morbidity, as indicated by their weight retention as compared to control mice (Fig. 1A). Furthermore, when we measured the viral load in each group we found that in parallel with weight retention, both *Pneumocystis*-recovered mice, and VLP-primed mice cleared the influenza virus to a significantly higher degree than control mice, despite their lack of previous exposure to influenza-specific antigens (Figs. 1B&C). These results suggested that very early innate immune events are key to enhanced downstream viral clearance in the lungs of both *Pneumocystis*- and VLP-primed mice.

Early local DC responses and accelerated trafficking to the TBLN are elicited by both infection with *Pneumocystis*, and exposure of the lungs to VLPs

Sentinel respiratory DCs are the first line of airway defense, sampling inhaled antigen and thereby initiating primary immune responses. Indeed, we have found previously that VLP-exposure of mice accelerates the onset of the primary antibody response upon subsequent influenza infection [16, 23]. We therefore determined the influx and efflux patterns of respiratory DCs in response to influenza virus in VLP-primed, *Pneumocystis*-infected, or the lungs of naïve mice. In comparison to DPBS controls, in mice that had been primed with either VLPs or *Pneumocystis*, both the lungs and TBLNs were populated with 1–2 $\log_{10}$ more DCs (defined as $CD11c^+Siglec\text{-}F^-$), even prior to infection (day 0) (Figs. 2A&B). However, in the case of both *Pneumocystis*-infected and VLP-exposed mice, the total quantity of DCs remained elevated over the course of the infection, whereas in the lungs, and more strikingly—in the TBLNs of DPBS mice, DCs were significantly delayed in achieving comparable numbers, suggesting a link between enhanced viral clearance and early DC presence in the effector site, as well as in the local lymph nodes.

We next phenotyped the participating DC populations in the lungs of VLP-exposed mice, at early timepoints post-influenza infection. Remarkably, both resident airway $CD103^+$ ($CD11c^+Siglec\text{-}F^-CD103^+CD11b^-$) and parenchymal $CD11b^+$ ($CD11c^+Siglec\text{-}F^-CD103^-CD11b^+$) [24–26] DCs in the lungs of VLP-exposed mice peaked in number, and we observed an efflux (which may be due to migration from the lungs into the TBLNs) between days 1 and 2 post-influenza infection (Figs. 2C–F). Furthermore, in VLP-exposed mice we observed a repeatable and sizable loss (or efflux) of both $CD103^+$ and $CD11b^+$ DCs from the TBLNs between 12 and 24 hours, which was recovered over the subsequent 24 hours (Figs. 2D&F). As will be discussed later, such dynamic DC trafficking, or efflux/loss has been reported [27–29]; however, the underlying mechanisms governing the rapid decline in trafficking into the lymph node remain unclear. A similar pattern to VLP-exposed mice was observed for the $CD103^+$ DC population in the lungs of control mice, albeit at a lower magnitude (Fig. 2C) and in the TBLNs, while the pattern of expansion and efflux/loss of $CD103^+$ DCs in control mice trended similarly to VLP-exposed mice, the timing was

delayed until day 4 post-infection (Fig. 2D). Interestingly, $CD11b^+$ DCs in both the lungs and TBLNs of control mice did not display the same efflux/loss pattern as was observed in VLP-primed mice, and instead $CD11b^+$ DCs steadily accumulated in both sites over the 7-day infection (Figs. 2E&F).

Enhanced expression of VCAM-1 and ICAM-1 on DCs facilitates T cell co-stimulation and activation in VLP-exposed mice

Although not quintessential co-stimulatory molecules, vascular cell adhesion molecule-1 (VCAM-1) and intracellular adhesion molecule-1 (ICAM-1) expressed on DCs are required for the co-stimulation of T cells to facilitate proliferation [30–33] and form a functional immunological synapse [34–36]. We therefore additionally determined the expression patterns of both VCAM-1 and ICAM-1 on DCs from lungs or TBLNs of VLP-exposed or control mice. In the lungs of VLP-exposed mice the expression of both VCAM-1 and ICAM-1 were significantly upregulated at 12 hours post-influenza infection, indicating enhanced co-stimulatory/adhesion activity directly in the effector site (Fig. 2G). By 24 hours post-infection, both receptors were substantially down-regulated, perhaps indicating the declining need for such heightened expression. Conversely, the DCs of control mice achieved no such peak, and in fact displayed an opposite trend, as they continued to slowly and progressively up-regulate the expression of co-stimulatory/adhesion molecules throughout the course of the 7-day infection. In the TBLNs, we found that in VLP-primed mice VCAM-1 and ICAM-1 are already highly expressed at day 0 (uninfected), and furthermore, that the number of DCs expressing co-stimulatory/adhesion molecules declined over the course of infection, which was again an opposite response from control mice, whose lungs and TBLNs responded very similarly (Fig. 2H). These results were consistent with the early loss of DC numbers from the TBLN of VLP-instilled mice as seen in Figs. 2D and F. Taken together, the accelerated rate of DC migration and the resultant enhanced viral clearance in either VLP-exposed or *Pneumocystis*-infected mice indicated that the rapidity of the innate immune response to a primary influenza challenge is impacted by previous lung priming, regardless of the antigenic specificity.

Exposure of the lungs to VLPs, or infection with *Pneumocystis* causes enhanced antigen processing in response to an unrelated challenge

Since enhanced DC trafficking to sites of antigen presentation strongly correlated to the kinetics of viral clearance in VLP-primed mice, we sought to define the potential functional differences in the antigen uptake and processing capacity of DCs (and other resident antigen presenting cells) elicited by VLP- or *Pneumocystis*-exposure. As above, we infected mice with *Pneumocystis* and allowed them to recover, or treated mice with VLPs, or vehicle prior to challenge with ovalbumin-DQ (OVA-DQ) or control ovalbumin (cold OVA) i.n. OVA-DQ is self-quenched in its native form and fluoresces only after it has been proteolytically cleaved, as is accomplished by antigen processing. We therefore were able to directly measure antigen uptake and processing by DCs and AMs in the lungs. Indeed, we found that both the DCs ($CD11c^+$Siglec-F^-) (Figs. 3A&B) and resident AMs ($CD11c^+$Siglec-F^+) (Figs. 3C&D) of VLP-primed mice took up and processed antigen with a faster rate and greater efficiency, thereby potentially allowing a jump-start in antigen clearance. In the lungs of VLP-treated mice, as early as 6 hours post-OVA-DQ instillation, DCs and AMs had already begun cleaving OVA-DQ, and this response peaked at 12 hours post-challenge. These events were unparalleled by control mice which never achieved the same level of antigen uptake and processing (Figs. 3A&C). Similarly, in the TBLNs of VLP-exposed mice DCs were highly active, processing antigen to a significantly higher degree than control mice, and clearing processed antigen (or potentially migrating from the site) already by 48 hours (Fig. 3B). AMs in the TBLNs of VLP-exposed mice exhibited less dramatic early differences. While the DCs and AMs of VLP-treated mice had mostly resolved their activity

by 48 hours post-OVA-DQ challenge (Figs. 3A-C), migratory macrophages in the TBLNs of control mice were finally able to achieve a similar peak of processing at 48 hours.

In the lungs of previously *Pneumocystis*-infected mice we found a slightly different pattern of antigen processing kinetics for both DCs and AMs (Figs. 3E&G). The most important timepoints for enhanced antigen processing for DCs in previously *Pneumocystis*-infected mice were between 24 and 48 hours (Fig. 3E). However, AMs showed no significant enhancements in antigen processing in the lungs (Fig. 3G). DCs and AMs in the TBLNs were similar to those of VLP-exposed mice (Figs. 3F&H). Therefore, not only were both the DCs and AMs in the primed lungs exhibiting alternative and accelerated trafficking patterns, they were also functionally enhanced.

We repeated these studies in VLP-exposed mice using an influenza-GFP [37] model to recapitulate these events in an infected lung (Supplemental Fig. S1). Similar to what we observed using OVA-DQ, total $CD11c^+$ cells (including both DCs and AMs) in the lung interstitium of VLP-exposed mice took up the NS1-GFP PR8 virus more rapidly and quickly degraded the GFP signal (Supplemental Fig. S1A). This could have been due to VLP-mediated enhanced resistance of these cells, or rapid uptake, processing, and clearance of the NS1-GFP PR8 virus. $CD11c^+$ cells of control mice incurred a protracted viral clearance process, resulting in a peak in the GFP signal at day 4. A similar pattern was observed in the airway spaces, as implicated by bronchoalveolar lavage (BAL) samples, again indicating the importance of the contributions from primed AMs (Supplemental Fig. S1B).

VLP-exposure alters the activity of $CD11c^+$ cells to provide downstream protective responses against influenza virus

Because we found that both trafficking and antigen processing were accelerated in VLP-exposed mice we next determined whether the observed enhancements of DC and AM function were required for the accelerated viral clearance. We therefore treated CD11c-diptheria toxin receptor transgenic (CD11c-DTR) [38, 39] or wild-type (WT) mice with VLPs, or DPBS, and allowed them to rest for 72 hours. We then administered 100 ng diphtheria toxin intratracheally (i.t.) to all groups to deplete total $CD11c^+$ cells (both DCs and AMs) from CD11c-DTR mice (Supplemental Figure S2A). Finally, we allowed new DCs and AMs to reestablish in the lungs by resting the mice for 9 days. Some of the mice were euthanized before influenza infection to determine the efficiency of $CD11c^+$ cell repopulation (Supplemental Figures S2B&C), whereas the remaining mice were euthanized at 7 days after infection to determine viral load (Figs. 4A&B). Thus, we created fully immunocompetent mice, which had been treated with VLPs, but which contained DCs and AMs that had accumulated in the lungs in the absence of VLPs, and thus lacked primed $CD11c^+$ cells which are normally present in the VLP-exposed mice. Functionally, we found that the mice repopulated with naïve $CD11c^+$ cells had lost the enhanced protection from viral challenge afforded by the VLP-exposure (Fig. 4A), and furthermore, that the expected serum IgG levels in reconstituted mice were significantly muted (Fig. 4B). Thus, we next determined how interfering with the migration of precursors to $CD11c^+$ cells contributed to the observed protection in VLP-treated mice.

Ly-$6C^+$ monocytes are more abundant in the lungs of antigen-exposed mice

Peripheral Ly-6C-expressing monocytes migrate into the lung to repopulate $CD11c^+$ cells (destined to become both DCs and AMs) [40] during homeostatic cellular turnover, and especially during infection. Given that we found that CD11c-priming was of the utmost importance to ensure protection against subsequent pathogen challenge via *Pneumocystis*-infection or VLP-exposure, we also determined the role for Ly-$6C^+$ precursors. In the lungs of both mice which had been previously infected with *Pneumocystis*, and those which had

been exposed to VLPs we found a significantly increased quantity of Ly-6C$^+$ cells prior to infection with influenza (Fig. 5A). Notably, in the lungs of *Pneumocystis*-infected mice these differences remained augmented throughout the course of infection.

Whereas simple repopulation may explain part of the role for Ly-6C$^+$ cells, we additionally determined their effector function through intracellular cytokine staining for TNF-α and iNOS. Importantly, we found that similarly to the total Ly-6C-expressing monocyte population, there was an increased abundance of TNF-α/iNOS-producing Ly-6C^{hi}CD11b$^+$ cells (often referred to as TipDCs) in both the lungs and TBLNs of both *Pneumocystis*-infected, and VLP-exposed mice (Figs. 5B&C), suggesting important effector functions for Ly-6C^{hi} cells.

Ccr2$^{-/-}$ mice are not protected from influenza virus via prior exposure to VLPs, or *Pneumocystis* infection

We next determined the necessity for Ly-6C^{hi} cells in enhancing the clearance of influenza virus in the lungs of previously *Pneumocystis*-infected or VLP-primed *Ccr2*$^{-/-}$ mice, as Ly-6C$^+$ cells in *Ccr2*$^{-/-}$ mice are impaired in trafficking to the site of infection. Interestingly, we found that neither VLP-primed, nor *Pneumocystis*-infected *Ccr2*$^{-/-}$ mice achieved heightened resistance to influenza infection as compared to controls (Figs. 6A–D). We also characterized the trafficking patterns of Ly-6C^{hi}CD11b$^+$ cells in VLP-exposed *Ccr2*$^{-/-}$ mice and found striking differences between *Ccr2*$^{-/-}$ mice and WT mice in numbers of recruited Ly-6C^{hi}CD11b$^+$ monocytes. In the BAL fluid (Fig. 6E), lungs (Fig. 6F) and TBLNs (Fig. 6G), we found that regardless of treatment with VLPs, *Ccr2*$^{-/-}$ mice lacked migratory Ly-6C^{hi}CD11b$^+$ monocytes (as has been reported [41, 42]). Additionally, only in WT VLP-primed mice did we find recruited Ly-6C^{hi}CD11b$^+$ monocytes in the TBLNs over the first 48 hours of infection (Fig. 6G). Finally, we determined the influenza-specific antibody concentration in the lavage fluid of VLP-, *Pneumocystis*-exposed, and control WT or *Ccr2*$^{-/-}$ mice. Importantly, we found that *Ccr2*$^{-/-}$ mice are additionally impaired in the production of high-titer antibody, despite their previous exposure to VLPs or *Pneumocystis* (Figs. 6H&I). Taken together, these results place importance on the effector function, efficient trafficking, and likely the direct exposure to priming antigens of Ly-6C$^+$ cells for the downstream protection against influenza virus in both VLP-exposed and *Pneumocystis*-infected mice. Specifically, while the influx of Ly-6C$^+$ cells after influenza infection is not sufficient for enhanced protection, our data (Fig. 6E) indicate that their influx in response to antigen priming prior to infection is required.

Discussion

Our understanding of the mechanisms by which remarkably divergent responses to identical pathogens may occur at the individual level, based upon past exposure events, remains to be fully developed. In our current studies, we have described a model of innate imprinting by which the instillation of VLPs, or a previous infection with *Pneumocystis*, both of which bear no antigenic similarity to influenza virus, protected naïve mice against subsequent high-dose influenza challenge. Importantly, differential DC trafficking was associated with the accelerated onset of the primary immune response. DCs are known to be essential to both influenza virus clearance [43] and the maintenance of inducible bronchus-associated lymphoid tissue (iBALT) [44, 45], which we have previously shown is a result of VLP-exposure [16], and *Pneumocystis* infection (unpublished observation). Additionally, viral infection is known to increase the number and rate of DC trafficking from the lungs to the lymph node, which is especially dynamic at early stages of infection [27, 46]. Consistent with the literature, we observed an accumulation of DCs (both airway and parenchymal) into the TBLNs after influenza infection, and even higher numbers accumulating in either VLP-

exposed or *Pneumocystis*-infected mice post-influenza infection. In addition, we observed a quick loss and recovery of DCs in TBLNs, which was much more pronounced in VLP-exposed mice. Thus, our model of innate imprinting altered the tempo of normal DC trafficking in response to influenza virus challenge, by accelerating and augmenting normal DC responses in VLP-exposed and *Pneumocystis*-infected mice. Finally, $CD103^+$ DCs have been shown to be not only most permissive to influenza infection, but also best at activating T cells in the lymph node [47, 48]. As is suggested here by our data and others [26], the accelerated presence and migration of the $CD103^+$ population may represent an important contribution to enhanced viral immunity. Importantly, we also found that VLP-exposed DCs display a differential pattern of T cell co-stimulatory/adhesion molecules in both the lungs and TBLNs. The very early (within 12 hours of infection) upregulation of VCAM-1 and ICAM-1 likely facilitated the formation of immunological synapses, allowing a potential jump-start in $CD4^+$ T cell expansion. Of note, (and not surprisingly) we have shown elsewhere that downstream $CD4^+$ T cell responses are ultimately required for the clearance of influenza virus [16] and Richert *et al*., Lymph Res and Biol, in press.

Either VLP-exposure or *Pneumocystis*-infection not only accelerated the rate of DC migration into the TBLNs, but also enhanced the antigen processing capacity of both DCs and AMs, as demonstrated by the accelerated processing of OVA-DQ. AMs are known to be important in antigen translocation from the airways [49, 50], and in maintenance of homeostasis in a steady state lung. Whereas AMs generally express a suppressive function, they may play a dynamic role in initiating, or controlling inflammation [51]. Additionally, the pathogen exposure history of DCs and AMs may be long-lasting and provide innate imprinting/memory [2, 10] and in this regard, we have previously observed protection afforded by VLP exposure to last for several weeks after cessation of VLP administration [16].

We found that VLP-exposure directly impacted the ability of $CD11c^+$ cells to react to downstream challenges, and in fact, that naïve $CD11c^+$ cells were unable to achieve a similar result when faced with influenza virus challenge. This was indicated by our finding that mice exposed to VLPs, subsequently depleted of $CD11c^+$ cells and allowed to be repopulated with naive $CD11c^+$ cells, lost the protective imprinting phenotype. Thus, the mechanism of innate imprinting in these studies was dependent on the priming of $CD11c^+$ cells (possibly both DCs and AMs).

A third population of antigen presenting cells, Ly-$6C^{hi}CD11b^+$ expressing monocytes (many of which were TipDCs) also appeared to be important in the enhanced viral clearance in our model. To the best of our knowledge, the functional contributions and trafficking of Ly-$6C^{hi}CD11b^+$ monocytes/TipDCs have not been determined in relation to innate imprinting. Here we found that in the absence of Ly-$6C^{hi}CD11b^+$ cells (in *Ccr2*$^{-/-}$ mice) the protection against influenza from previous *Pneumocystis*-infection or VLP-exposure, was lost. This protection appeared to be partially dependent on the accelerated early contribution, and possibly the presence of these cells in the effector site and contact with antigen. Importantly, Ly-$6C^{hi}CD11b^+$ cells are highly multifunctional and may situationally promote or discourage inflammation [40, 52–55]. Thus, Ly-$6C^{hi}CD11b^+$ cells could have been important to VLP/*Pneumocystis*-enhanced viral clearance, through the repopulation of antigen presenting cells (APC's) into the effector sites, through promoting T cell activation via their APC function [52, 53], or by dampening late T cell responses to control damage through the production of nitric oxide (NO) [53, 56]. Additionally, we found that local antibody production in *Ccr2*$^{-/-}$ mice is blunted, despite VLP-exposure, thus further suggesting a reliance of downstream adaptive immune responses on efficient Ly-6C-cell mediated function. Importantly, while there is some debate about the necessity for CCR2-dependent signaling in the clearance of influenza and control of morbidity [52, 54, 55], we

find that proficient CCR2-signaling is imperative to the accelerated influenza virus clearance in VLP-exposed or *Pneumocystis*-infected mice. Others have similarly reported the necessity for early CCR2-dependent trafficking of Ly-6C-expressing cells in the clearance of pathogens including *Mycobacterium tuberculosis* [57], *Cryptococcus neoformans* [58], and *Listeria monocytogenes* [59].

In conclusion, we have herein illustrated a mechanism by which we can harness the pulmonary mucosa to provide accelerated site-specific immunity to a primary challenge with a completely immunologically disparate pathogen/antigen. Furthermore, our results suggest that the utilization of non-infectious and non-replicating VLPs, sharing no cross-reactive epitopes to influenza, may provide a novel model by which we may begin to better understand the complex interplay between lung priming, heterologous immunity, innate imprinting, and memory responses. This system could be particularly advantageous in that, unlike primary pathogen challenge models, no damage to the epithelium, or pulmonary function occurs by VLP-priming.

Materials and Methods

Virus-like particle production and purification

Virus-like particles (small heat-shock protein cage nanoparticles G41C) were produced, purified, and characterized as previously described [16, 60].

Pathogens

The influenza virus A/PR8/8/34 was produced at the Trudeau Institute (Saranac Lake, NY). Briefly, 10 day old embryonated chicken eggs were infected for 55 hours, and resultant allantoic fluid was recovered and stored at −80° C until used.

Pneumocystis murina was maintained in infected SCID mice. At the time of infection, one or more donor mouse was euthanized and whole lung homogenate was sterilely collected and washed. *Pneumocystis* was then enumerated, and used in infections.

Animals and *in vivo* procedures

Female or male BALB/c, C57BL/6, *Ccr2*$^{-/-}$, or CD11c-DTR [38, 39] mice were bred in-house at Montana State University, maintained in SPF conditions in HEPA-filtered cages, and fed sterile food and water *ad libitum*. All animal procedures were performed in accordance with protocols pre-approved by the Montana State University Institutional Animal Care and Use Committee (IACUC).

VLPs, *Pneumocystis* infection, and influenza were delivered to mice lightly anesthetized with 5% inhaled isoflurane. VLP-treatment was delivered in five intranasal (i.n.) doses of 100 μg (50 μl) given either daily, or spaced 3 days apart (both schedules produced equivalent results). Mice were then rested for 72 hours before challenge or further manipulation. *Pneumocystis* infections were performed by delivering 10^7 organisms in 100 μl volumes intratracheally (i.t.) two weeks prior to challenge with influenza. Required rest time between priming and influenza infection for each scenario was previously established due to peak immune responsiveness. For influenza challenges 1.5×10^3 plaque-forming units (pfu) (1 LD_{50}) PR8 was delivered in 50 μl volumes i.n. In some experiments, mice were challenged with 100 μg Ovalbumin-DQ (Molecular Probes; Carlsbad, CA) or regular “cold” OVA (Sigma-Aldrich; St. Louis, MO) in 50 μl i.n. For experiments using CD11c-DTR-facilitated depletion, anesthetized mice received an i.t. instillation of 100 ng diphtheria toxin (DT) (Sigma-Aldrich) in 100 μl sterile DPBS. At indicated timepoints per experiment,

mice were euthanized by i.p. injection of sodium pentobarbital (90 mg/kg) and exsanguinated after no pedal response could be elicited.

Bronchoalveolar lavage (BAL) samples were collected by instilling the lung with 2 mL DPBS with 3 mM EDTA. Resultant cells were spun at 209 × g for 10 minutes at 4°C and supernatants were collected for further assay. Pellets were then resuspended in FcR block (clone 93) prior to staining for FACS. Lungs were excised and either snap frozen in 2 mL DMEM for plaque assay to determine viral load, or digested in 0.2% collagenase (Worthington Biochemical Corporation; Lakewood, NJ) with 0.1% DNase (Sigma-Aldrich) in RPMI with agitation at 37° C for 1 hr. Red blood cells were lysed from the lung homogenates using ACK lysis buffer. Remaining cells were washed, resuspended in FcR block, and stained for flow cytometry. Tracheobronchial lymph nodes (TBLNs) were either homogenized through a wire mesh screen to collect lymphocytes or digested in collagenase media to collect macrophages and DCs. Total cells from each tissue were counted by hemocytometer to allow for total quantification by FACS.

FACS staining and antibodies

Single-cell suspensions from indicated organs were filtered through 100 μM mesh, and incubated with FcR block (clone 93) for 10 minutes on ice. Antibody cocktails were then added and the cells were incubated on ice for an additional 20–30 minutes. Antibodies purchased from Biolegend (San Diego, CA) included CD11c-PerCP-Cy5.5 (clone N418); CD103-APC (clone 2E7); CD11b-APC-Cy7 (clone M1/70); I-A/I-E-PE-Cy7 (M5/114.15.2); Ly-6C-FITC (clone HK1.4); ICAM-1-APC (clone YN1/1.7.4); andVCAM-1-PerCP-Cy5.5 (clone 429 (MVCAM.A)). Siglec-F-PE (clone E50-2440) and iNOS-FITC (clone 6/iNOS/NOS Type II) were purchased from BD biosciences (San Jose, CA). TNF-α-AF647 (clone MP6-XT22), and isotype controls (clones eBRG1 and eBR2a) were purchased from eBioscience.

Samples were acquired on a FACSCanto (BD) and data was analyzed using FlowJo software (Treestar; Ashland, OR). Briefly, forward and side scatter plots were gated on the population of interest (DCs/macrophages) as determined by size and granularity. Cells were then further analyzed for the expression of appropriate combinations of surface antigens based off negative staining or isotype controls. Total cell numbers were then calculated based off total hemocytometer cell counts.

ELISA

BALF antibodies levels were determined by ELISA. Briefly, high-binding plates (Corning; Corning, NY) were incubated with influenza virus membrane. Plates were then washed, and blocked. BALF samples were plated in duplicate and incubated at 37°C for 2 hrs. Plates were again washed and alkaline phosphatase-conjugated IgG (Sigma-Aldrich) were added and incubated again. Finally, plates were again washed, developed with 4-Nitrophenyl phosphate disodium salt hexahydrate (Sigma-Aldrich) in diethanolamine buffer, and read on a SpectraMax Plus plate reader (Molecular Devices; Sunnyvale, CA) at 405 nm.

Viral Quantification

Plaque assay was used to determine viral titers from total lung homogenate, as previously described [16]. Briefly, Madin-Darby canine kidney (MDCK) cells were grown to confluence. Next, 10-fold serial dilutions of total lung homogenate were plated onto the monolayer, and the assay was overlayed with 1.2% agarose with DEAE. The assay was incubated at 35° C in the presence of CO_2 for 3–5 days. It was then fixed with 20% acetic acid and stained with 0.2% crystal violet.

Statistics

Statistical significance was determined by either a One-way ANOVA with a Bonferroni's post-test of multiple comparisons, or an unpaired *t*-test using GraphPad Prism (La Jolla, CA). Significance was indicated by * $P<.05$, ** $P<.01$, *** $P<.001$, or **** $P<.0001$ (or corresponding numbers of alternative symbols, as indicated per figure legend). Figure legends disclose the use of statistics in each scenario. Figures are representative of one independent experiment (n=5 mice per group) and error bars represent the standard error of the mean (SEM).

Supplementary Material

Refer to Web version on PubMed Central for supplementary material.

Acknowledgments

We thank Dr. Adolfo García-Sastre for his generous gift of the NS1-GFP virus, all Harmsen lab staff for technical assistance in experiments, Amy Servid for producing and purifying the VLPs, and the staff of Montana State University's Animal Resource Center for animal care and technical aid. This work was supported by NIH/NIAID R01 AI104905 (AGH and TD) NIH/NIAID R56AI089458 (AGH); NIH R01-EB012027 (TD); NIH/NIAID R21AI083520 (JAW); the Rocky Mountain Research Center of Excellence (RMRCE) U54AI065357 (John T. Belisle); the IDeA Network for Biomedical Research Excellence (INBRE) P20GM103474 (AGH); the Center for Zoonotic and Emerging Infectious Diseases (COBRE) P20GM103500 (Mark T. Quinn); the M.J. Murdock Charitable Trust, and the Montana State University Agricultural Experimental Station.

Abbreviations used in this article

AM	Alveolar Macrophage
VLPs	virus-like particles
TBLN	tracheobronchial lymph node

References

1. Wiley JA, Harmsen AG. Pneumocystis infection enhances antibody-mediated resistance to a subsequent influenza infection. J Immunol. 2008; 180:5613–5624. [PubMed: 18390746]
2. Goulding J, Snelgrove R, Saldana J, Didierlaurent A, Cavanagh M, Gwyer E, Wales J, Wissinger EL, Hussell T. Respiratory infections: do we ever recover? Proc Am Thorac Soc. 2007; 4:618–625. [PubMed: 18073393]
3. Walzl G, Tafuro S, Moss P, Openshaw PJ, Hussell T. Influenza virus lung infection protects from respiratory syncytial virus-induced immunopathology. J Exp Med. 2000; 192:1317–1326. [PubMed: 11067880]
4. Wissinger E, Goulding J, Hussell T. Immune homeostasis in the respiratory tract and its impact on heterologous infection. Semin Immunol. 2009; 21:147–155. [PubMed: 19223202]
5. Kamradt T, Goggel R, Erb KJ. Induction, exacerbation and inhibition of allergic and autoimmune diseases by infection. Trends Immunol. 2005; 26:260–267. [PubMed: 15866239]
6. Nie S, Lin SJ, Kim SK, Welsh RM, Selin LK. Pathological features of heterologous immunity are regulated by the private specificities of the immune repertoire. Am J Pathol. 2010; 176:2107–2112. [PubMed: 20348239]
7. Welsh RM, Che JW, Brehm MA, Selin LK. Heterologous immunity between viruses. Immunol Rev. 2010; 235:244–266. [PubMed: 20536568]
8. Chen HD, Fraire AE, Joris I, Brehm MA, Welsh RM, Selin LK. Memory CD8+ T cells in heterologous antiviral immunity and immunopathology in the lung. Nat Immunol. 2001; 2:1067–1076. [PubMed: 11668342]

9. Selin LK, Brehm MA, Naumov YN, Cornberg M, Kim SK, Clute SC, Welsh RM. Memory of mice and men: CD8+ T-cell cross-reactivity and heterologous immunity. Immunol Rev. 2006; 211:164–181. [PubMed: 16824126]
10. Mackaness GB. The Immunological Basis of Acquired Cellular Resistance. J Exp Med. 1964; 120:105–120. [PubMed: 14194388]
11. Rynda-Apple A, Dobrinen E, McAlpine M, Read A, Harmsen A, Richert LE, Calverley M, Pallister K, Voyich J, Wiley JA, Johnson B, Young M, Douglas T, Harmsen AG. Virus-like particle-induced protection against MRSA pneumonia is dependent on IL-13 and enhancement of phagocyte function. Am J Pathol. 2012; 181:196–210. [PubMed: 22642909]
12. Kim KK, Kim R, Kim SH. Crystal structure of a small heat-shock protein. Nature. 1998; 394:595–599. [PubMed: 9707123]
13. Kim R, Kim KK, Yokota H, Kim SH. Small heat shock protein of Methanococcus jannaschii, a hyperthermophile. Proc Natl Acad Sci U S A. 1998; 95:9129–9133. [PubMed: 9689045]
14. Flenniken ML, Willits DA, Brumfield S, Young MJ, Douglas T. The small heat shock protein cage from Methanococcus jannaschii is a versatile nanoscale platform for genetic and chemical modification. Nano Letters. 2003; 3:1573–1576.
15. Kaiser CR, Flenniken ML, Gillitzer E, Harmsen AL, Harmsen AG, Jutila MA, Douglas T, Young MJ. Biodistribution studies of protein cage nanoparticles demonstrate broad tissue distribution and rapid clearance in vivo. Int J Nanomedicine. 2007; 2:715–733. [PubMed: 18203438]
16. Wiley JA, Richert LE, Swain SD, Harmsen A, Barnard DL, Randall TD, Jutila M, Douglas T, Broomell C, Young M. Inducible Bronchus-associated lymphoid tissue elicited by a protein cage nanoparticle enhances protection in mice against diverse respiratory viruses. PLoS One. 2009; 4:e7142. [PubMed: 19774076]
17. Introini A, Vanpouille C, Lisco A, Grivel JC, Margolis L. Interleukin-7 facilitates HIV-1 transmission to cervico-vaginal tissue ex vivo. PLoS Pathog. 2013; 9:e1003148. [PubMed: 23408885]
18. Foo SY, Phipps S. Regulation of inducible BALT formation and contribution to immunity and pathology. Mucosal Immunol. 2010; 3:537–544. [PubMed: 20811344]
19. Holt PG. Development of bronchus associated lymphoid tissue (BALT) in human lung disease: a normal host defence mechanism awaiting therapeutic exploitation? Thorax. 1993; 48:1097–1098. [PubMed: 8296250]
20. Holt PG, Strickland DH, Wikstrom ME, Jahnsen FL. Regulation of immunological homeostasis in the respiratory tract. Nat Rev Immunol. 2008; 8:142–152. [PubMed: 18204469]
21. Pabst R, Tschernig T. Bronchus-associated lymphoid tissue: an entry site for antigens for successful mucosal vaccinations? Am J Respir Cell Mol Biol. 2010; 43:137–141. [PubMed: 20508066]
22. Hussell T, Goulding J. Structured regulation of inflammation during respiratory viral infection. Lancet Infect Dis. 2010; 10:360–366. [PubMed: 20417418]
23. Richert LE, Servid AE, Harmsen AL, Rynda-Apple A, Han S, Wiley JA, Douglas T, Harmsen AG. A virus-like particle vaccine platform elicits heightened and hastened local lung mucosal antibody production after a single dose. Vaccine. 2012
24. Beaty SR, Rose CE Jr, Sung SS. Diverse and potent chemokine production by lung CD11bhigh dendritic cells in homeostasis and in allergic lung inflammation. J Immunol. 2007; 178:1882–1895. [PubMed: 17237439]
25. Sung SS, Fu SM, Rose CE Jr, Gaskin F, Ju ST, Beaty SR. A major lung CD103 (alphaE)-beta7 integrin-positive epithelial dendritic cell population expressing Langerin and tight junction proteins. J Immunol. 2006; 176:2161–2172. [PubMed: 16455972]
26. Hao X, Kim TS, Braciale TJ. Differential response of respiratory dendritic cell subsets to influenza virus infection. J Virol. 2008; 82:4908–4919. [PubMed: 18353940]
27. Legge KL, Braciale TJ. Accelerated migration of respiratory dendritic cells to the regional lymph nodes is limited to the early phase of pulmonary infection. Immunity. 2003; 18:265–277. [PubMed: 12594953]
28. Randolph GJ, Angeli V, Swartz MA. Dendritic-cell trafficking to lymph nodes through lymphatic vessels. Nat Rev Immunol. 2005; 5:617–628. [PubMed: 16056255]

29. Cook DN, Bottomly K. Innate immune control of pulmonary dendritic cell trafficking. Proc Am Thorac Soc. 2007; 4:234–239. [PubMed: 17607005]
30. van Seventer GA, Newman W, Shimizu Y, Nutman TB, Tanaka Y, Horgan KJ, Gopal TV, Ennis E, O'Sullivan D, Grey H, et al. Analysis of T cell stimulation by superantigen plus major histocompatibility complex class II molecules or by CD3 monoclonal antibody: costimulation by purified adhesion ligands VCAM-1, ICAM-1, but not ELAM-1. J Exp Med. 1991; 174:901–913. [PubMed: 1717633]
31. Damle NK, Aruffo A. Vascular cell adhesion molecule 1 induces T-cell antigen receptor-dependent activation of CD4+T lymphocytes. Proc Natl Acad Sci U S A. 1991; 88:6403–6407. [PubMed: 1713678]
32. Damle NK, Klussman K, Linsley PS, Aruffo A. Differential costimulatory effects of adhesion molecules B7, ICAM-1, LFA-3, and VCAM-1 on resting and antigen-primed CD4+ T lymphocytes. J Immunol. 1992; 148:1985–1992. [PubMed: 1372018]
33. Lebedeva T, Dustin ML, Sykulev Y. ICAM-1 co-stimulates target cells to facilitate antigen presentation. Curr Opin Immunol. 2005; 17:251–258. [PubMed: 15886114]
34. Mittelbrunn M, Molina A, Escribese MM, Yanez-Mo M, Escudero E, Ursa A, Tejedor R, Mampaso F, Sanchez-Madrid F. VLA-4 integrin concentrates at the peripheral supramolecular activation complex of the immune synapse and drives T helper 1 responses. Proc Natl Acad Sci U S A. 2004; 101:11058–11063. [PubMed: 15263094]
35. Grakoui A, Bromley SK, Sumen C, Davis MM, Shaw AS, Allen PM, Dustin ML. The immunological synapse: a molecular machine controlling T cell activation. Science. 1999; 285:221–227. [PubMed: 10398592]
36. Carrasco YR, Batista FD. B-cell activation by membrane-bound antigens is facilitated by the interaction of VLA-4 with VCAM-1. EMBO J. 2006; 25:889–899. [PubMed: 16456548]
37. Manicassamy B, Manicassamy S, Belicha-Villanueva A, Pisanelli G, Pulendran B, Garcia-Sastre A. Analysis of in vivo dynamics of influenza virus infection in mice using a GFP reporter virus. Proc Natl Acad Sci U S A. 2010; 107:11531–11536. [PubMed: 20534532]
38. Jung S, Unutmaz D, Wong P, Sano G, De los Santos K, Sparwasser T, Wu S, Vuthoori S, Ko K, Zavala F, Pamer EG, Littman DR, Lang RA. In vivo depletion of CD11c+ dendritic cells abrogates priming of CD8+ T cells by exogenous cell-associated antigens. Immunity. 2002; 17:211–220. [PubMed: 12196292]
39. Bennett CL, Clausen BE. DC ablation in mice: promises, pitfalls, and challenges. Trends Immunol. 2007; 28:525–531. [PubMed: 17964853]
40. Dominguez PM, Ardavin C. Differentiation and function of mouse monocyte-derived dendritic cells in steady state and inflammation. Immunol Rev. 2010; 234:90–104. [PubMed: 20193014]
41. Serbina NV, Pamer EG. Monocyte emigration from bone marrow during bacterial infection requires signals mediated by chemokine receptor CCR2. Nat Immunol. 2006; 7:311–317. [PubMed: 16462739]
42. Tsou CL, Peters W, Si Y, Slaymaker S, Aslanian AM, Weisberg SP, Mack M, Charo IF. Critical roles for CCR2 and MCP-3 in monocyte mobilization from bone marrow and recruitment to inflammatory sites. J Clin Invest. 2007; 117:902–909. [PubMed: 17364026]
43. McGill J, Van Rooijen N, Legge KL. Protective influenza-specific CD8 T cell responses require interactions with dendritic cells in the lungs. J Exp Med. 2008; 205:1635–1646. [PubMed: 18591411]
44. Halle S, Dujardin HC, Bakocevic N, Fleige H, Danzer H, Willenzon S, Suezer Y, Hammerling G, Garbi N, Sutter G, Worbs T, Forster R. Induced bronchus-associated lymphoid tissue serves as a general priming site for T cells and is maintained by dendritic cells. J Exp Med. 2009; 206:2593–2601. [PubMed: 19917776]
45. GeurtsvanKessel CH, Willart MA, Bergen IM, van Rijt LS, Muskens F, Elewaut D, Osterhaus AD, Hendriks R, Rimmelzwaan GF, Lambrecht BN. Dendritic cells are crucial for maintenance of tertiary lymphoid structures in the lung of influenza virus-infected mice. J Exp Med. 2009; 206:2339–2349. [PubMed: 19808255]

46. Dahl ME, Dabbagh K, Liggitt D, Kim S, Lewis DB. Viral-induced T helper type 1 responses enhance allergic disease by effects on lung dendritic cells. Nat Immunol. 2004; 5:337–343. [PubMed: 14973436]
47. GeurtsvanKessel CH, Lambrecht BN. Division of labor between dendritic cell subsets of the lung. Mucosal Immunol. 2008; 1:442–450. [PubMed: 19079211]
48. GeurtsvanKessel CH, Willart MA, van Rijt LS, Muskens F, Kool M, Baas C, Thielemans K, Bennett C, Clausen BE, Hoogsteden HC, Osterhaus AD, Rimmelzwaan GF, Lambrecht BN. Clearance of influenza virus from the lung depends on migratory langerin+CD11b- but not plasmacytoid dendritic cells. J Exp Med. 2008; 205:1621–1634. [PubMed: 18591406]
49. Harmsen AG, Muggenburg BA, Snipes MB, Bice DE. The role of macrophages in particle translocation from lungs to lymph nodes. Science. 1985; 230:1277–1280. [PubMed: 4071052]
50. Kirby AC, Coles MC, Kaye PM. Alveolar macrophages transport pathogens to lung draining lymph nodes. J Immunol. 2009; 183:1983–1989. [PubMed: 19620319]
51. Goulding J, Godlee A, Vekaria S, Hilty M, Snelgrove R, Hussell T. Lowering the threshold of lung innate immune cell activation alters susceptibility to secondary bacterial superinfection. J Infect Dis. 2011; 204:1086–1094. [PubMed: 21881124]
52. Aldridge JR Jr, Moseley CE, Boltz DA, Negovetich NJ, Reynolds C, Franks J, Brown SA, Doherty PC, Webster RG, Thomas PG. TNF/iNOS-producing dendritic cells are the necessary evil of lethal influenza virus infection. Proc Natl Acad Sci U S A. 2009; 106:5306–5311. [PubMed: 19279209]
53. Zhu B, Kennedy JK, Wang Y, Sandoval-Garcia C, Cao L, Xiao S, Wu C, Elyaman W, Khoury SJ. Plasticity of Ly-6C(hi) myeloid cells in T cell regulation. J Immunol. 2011; 187:2418–2432. [PubMed: 21824867]
54. Lin KL, Suzuki Y, Nakano H, Ramsburg E, Gunn MD. CCR2+ monocyte-derived dendritic cells and exudate macrophages produce influenza-induced pulmonary immune pathology and mortality. J Immunol. 2008; 180:2562–2572. [PubMed: 18250467]
55. Lin KL, Sweeney S, Kang BD, Ramsburg E, Gunn MD. CCR2-antagonist prophylaxis reduces pulmonary immune pathology and markedly improves survival during influenza infection. J Immunol. 2011; 186:508–515. [PubMed: 21098218]
56. Deshane J, Zmijewski JW, Luther R, Gaggar A, Deshane R, Lai JF, Xu X, Spell M, Estell K, Weaver CT, Abraham E, Schwiebert LM, Chaplin DD. Free radical-producing myeloid-derived regulatory cells: potent activators and suppressors of lung inflammation and airway hyperresponsiveness. Mucosal Immunol. 2011; 4:503–518. [PubMed: 21471960]
57. Peters W, Scott HM, Chambers HF, Flynn JL, Charo IF, Ernst JD. Chemokine receptor 2 serves an early and essential role in resistance to Mycobacterium tuberculosis. Proc Natl Acad Sci U S A. 2001; 98:7958–7963. [PubMed: 11438742]
58. Osterholzer JJ, Chen GH, Olszewski MA, Curtis JL, Huffnagle GB, Toews GB. Accumulation of CD11b+ lung dendritic cells in response to fungal infection results from the CCR2-mediated recruitment and differentiation of Ly-6Chigh monocytes. J Immunol. 2009; 183:8044–8053. [PubMed: 19933856]
59. Serbina NV, Salazar-Mather TP, Biron CA, Kuziel WA, Pamer EG. TNF/iNOS-producing dendritic cells mediate innate immune defense against bacterial infection. Immunity. 2003; 19:59–70. [PubMed: 12871639]
60. Flenniken ML, Willits DA, Harmsen AL, Liepold LO, Harmsen AG, Young MJ, Douglas T. Melanoma and lymphocyte cell-specific targeting incorporated into a heat shock protein cage architecture. Chem Biol. 2006; 13:161–170. [PubMed: 16492564]

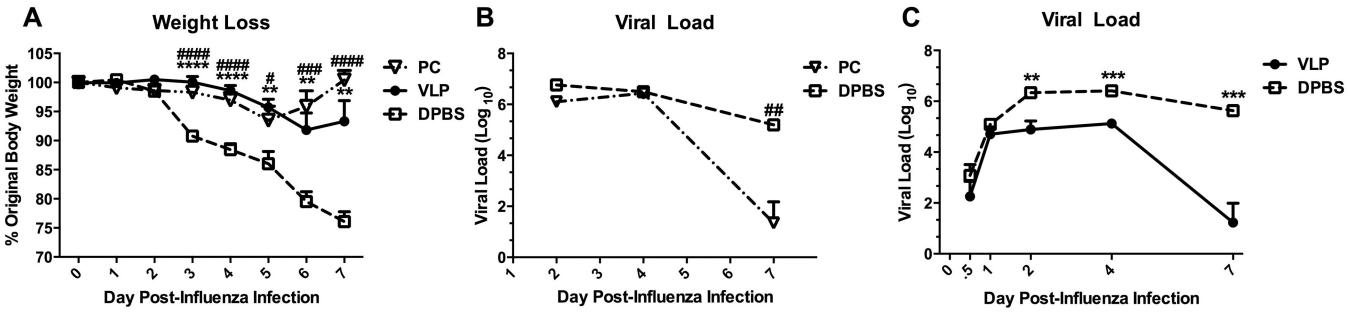

Figure 1.

Both natural infection with *Pneumocystis*, and the exposure of the lungs to non-replicative VLPs provide protection against morbidity, and enhance the clearance of an unrelated pathogen. Wild-type (BALB/c) mice were infected with 10^7 *Pneumocystis* organisms (PC) i.t. and were allowed to recover for two weeks (A&B). Two additional groups of mice were dosed once daily for 5 days with 100 μg/50 μl VLPs (or DPBS) i.n. and then rested for 72 hours (A-C). All mice were then infected with 1.5×10^3 pfu PR8 influenza virus, weighed daily (A), and sacrificed at indicated timepoints to determine viral load in the left lobe of the lung (B&C). Data are shown as mean + SEM of n=5. Experiments of similar design were independently performed at least twice. Significance as compared to the DPBS control group (unpaired *t*-test) is indicated by "#" for PC-infected mice and "*" for VLP-exposed mice.

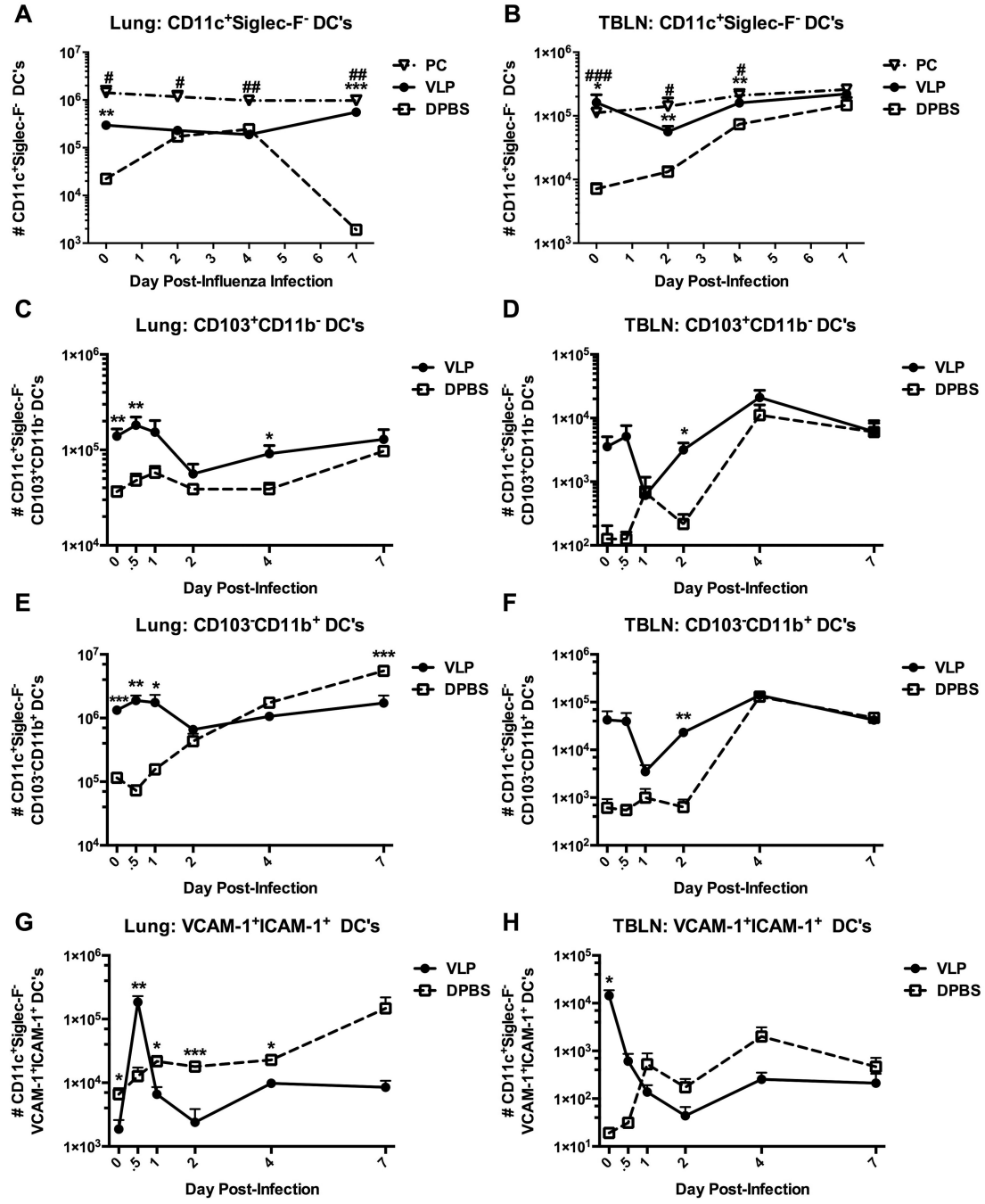

Figure 2.

Early local DC responses and accelerated trafficking to the TBLN are elicited by both infection with *Pneumocystis*, and exposure of the lungs to VLPs. Wild-type (BALB/c) mice were infected with *Pneumocystis* (PC), or were exposed to VLPs (A-H). All mice were then infected with 1.5×10^3 pfu PR8 influenza virus and sacrificed at indicated timepoints to determine dendritic cell populations present in the multilobe of the lungs and whole TBLN. Conventional DCs ($CD11c^+$Siglec-F) (A&B), resident airway DCs ($CD11c^+$Siglec-F$CD103^+CD11b$) (C&D), parenchymal/interstitial DCs ($CD11c^+$Siglec-F$CD103CD11b^+$) (E&F), and conventional DCs co-expressing VCAM-1 and ICAM-1 in both the lungs (left

panel) and TBLNs (right panel) were quantified by flow cytometry and total hemocytometer cell counts. Data are shown as mean + SEM of n=5. Experiments of similar design were independently performed at least twice. Significance as compared to the DPBS control group (unpaired *t*-test) is indicated by "#" for PC-infected mice and "*" for VLP-exposed mice.

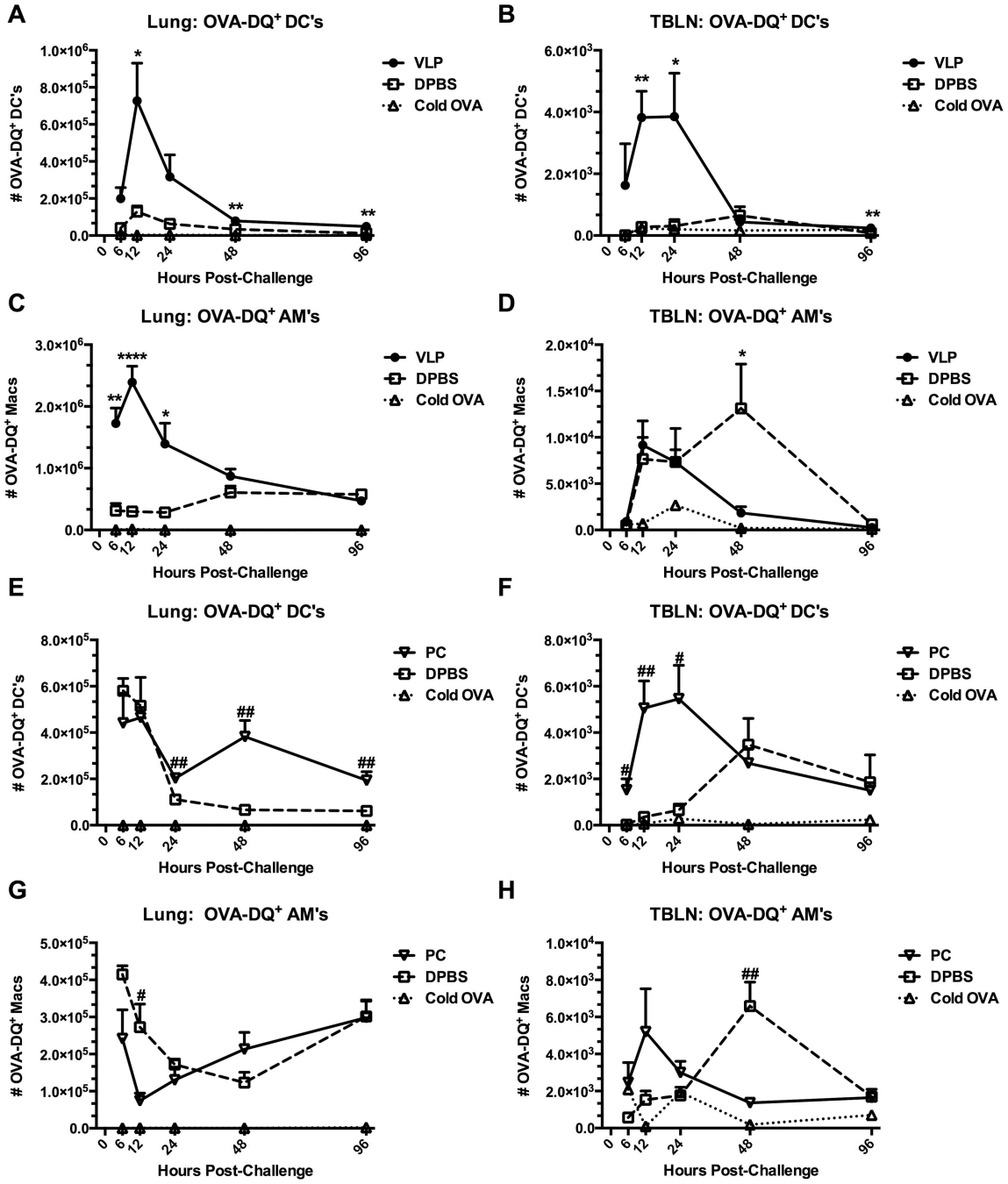

Figure 3.

Exposure of the lungs to VLPs, or infection with *Pneumocystis* causes enhanced antigen processing in response to an unrelated challenge. Mice were exposed to VLPs or vehicle (A-D) (C57BL/6), or infected with *Pneumocystis* (PC) (E-H) (BALB/c). Recovered mice were then i.n. challenged with 100 μg Ovalbumin-DQ, or unlabeled regular "cold" OVA as a staining control, and sacrificed at designated timepoints. OVA-DQ$^+$ DCs (A&B, E&F) and AMs (C&D, G&H) in whole lungs (left panel) and TBLNs (right panel) were quantified by FACS and total hemocytometer cell counts. DCs and AMs were identified as CD11c$^+$ and Siglec-F (DCs) or Siglec-F$^+$ (AMs) from plots previously gated on forward and side scatter. Total cells were additionally quantified by total hemocytometer counts. Data are shown as

mean + SEM of n=5. Experiments of similar design were independently performed at least twice. Significance as compared to the DPBS control group (unpaired *t*-test) is indicated by "#" for PC-infected mice and "*" for VLP-exposed mice.

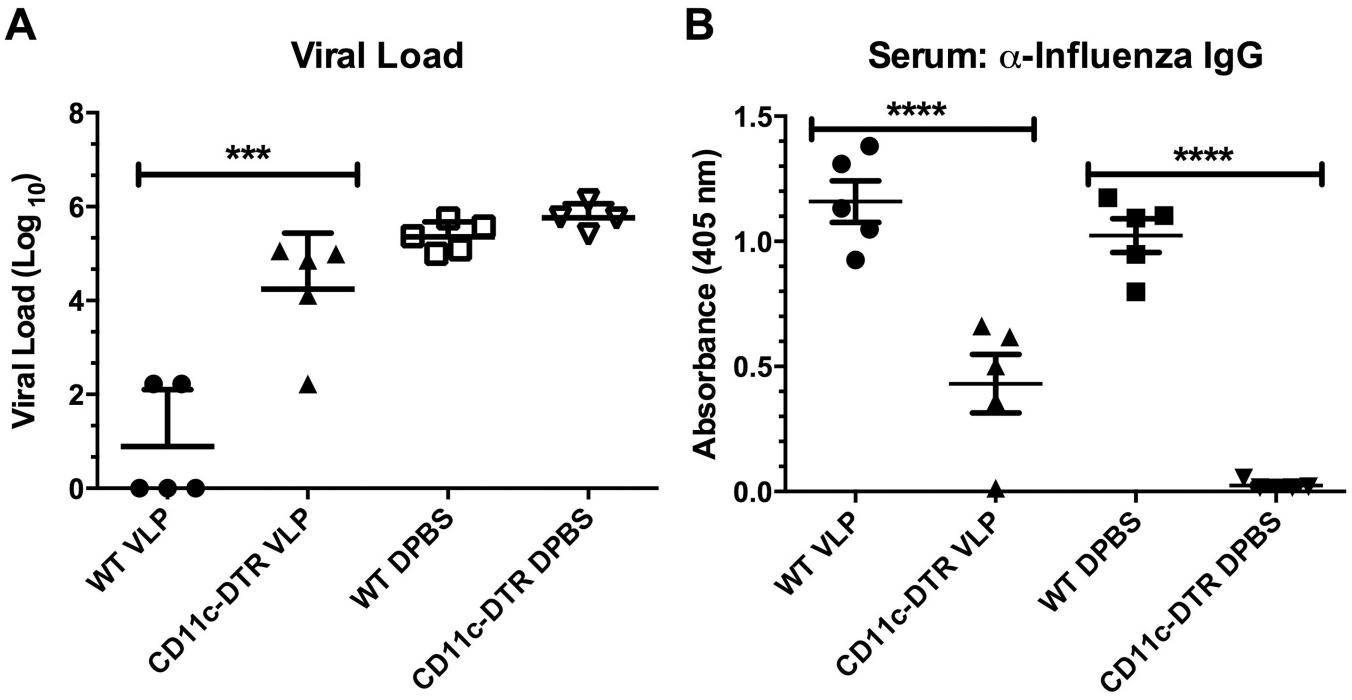

Figure 4.

VLP-exposure alters the activity of $CD11c^+$ cells. C57BL/6 (WT) or CD11c-DTR mice were exposed to VLPs or vehicle i.n., rested for 72 hours, and then treated with 100 ng diphtheria toxin (DT) i.t to deplete $CD11c^+$ cells from CD11c-DTR mice. Next, all groups were rested for 9 days to allow for $CD11c^+$ cell reconstitution from the bone marrow, and finally challenged with 1.5×10^3 pfu PR8 influenza. At day 7 post-infection mice were euthanized and the total viral load (A) was determined from the left lobe of the lung. Serum IgG (diluted at 1:50) was additionally assayed by antibody ELISA (B). Each experiment was independently repeated at least twice with n=5 per group. A one-way ANOVA followed by a Bonferroni's post-test between groups was utilized to determine statistical significance.

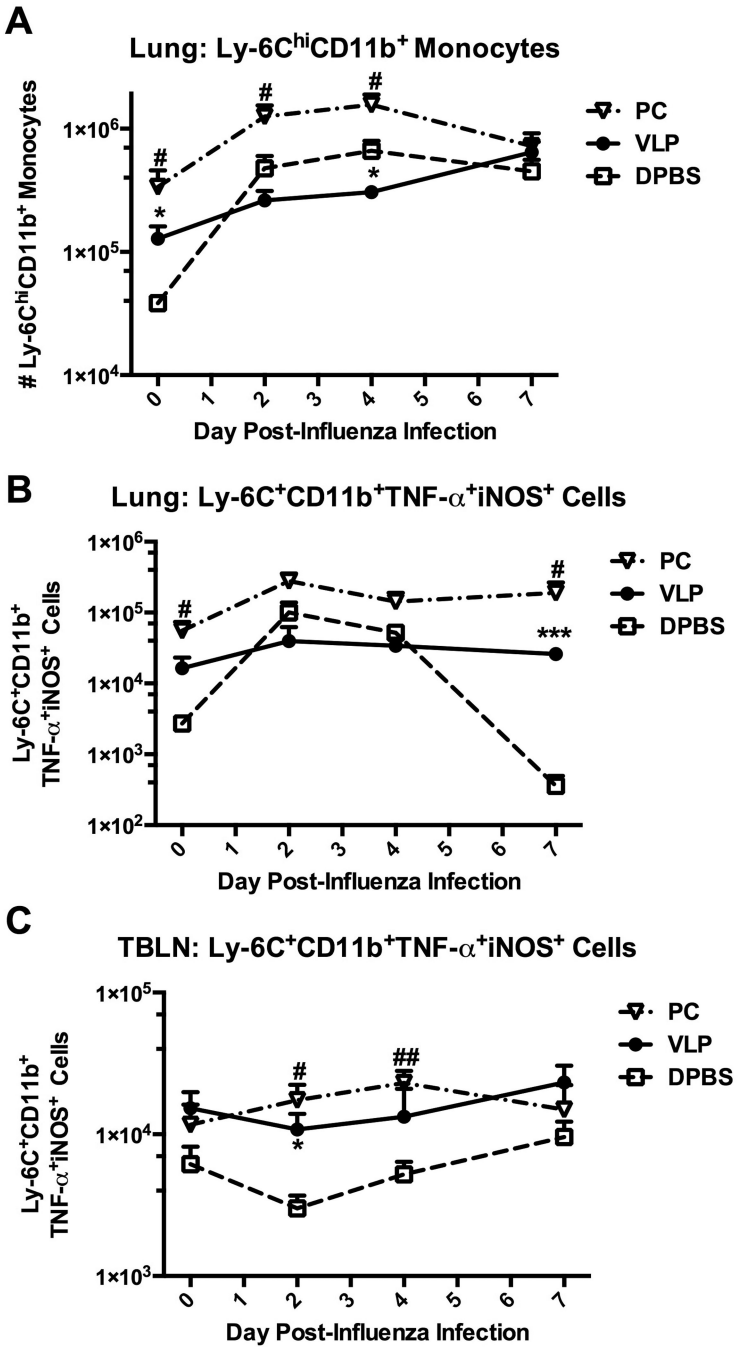

Figure 5.

Ly-6C$^+$ monocytes are more abundant in the lungs of antigen-exposed mice. Wild-type BALB/c mice were exposed to VLPs or vehicle, or infected with *Pneumocystis* (PC). Rested mice were then i.n. challenged with 1.5×10^3 pfu PR8 influenza virus and sacrificed at designated timepoints. Ly-6C^{hi}CD11b$^+$ (A) or Ly-6C$^+$CD11b$^+$TNF-α$^+$iNOS$^+$ (B&C) cells were quantified from the multilobe of the lungs (A&B) and TBLNs (C) by flow cytometry and hemocytometer cell counts. Data are shown as mean + SEM of n=5. Experiments of similar design were independently performed at least twice. Significance as compared to the

DPBS control group (unpaired *t*-test) is indicated by "#" for PC-infected mice and "*" for VLP-exposed mice.

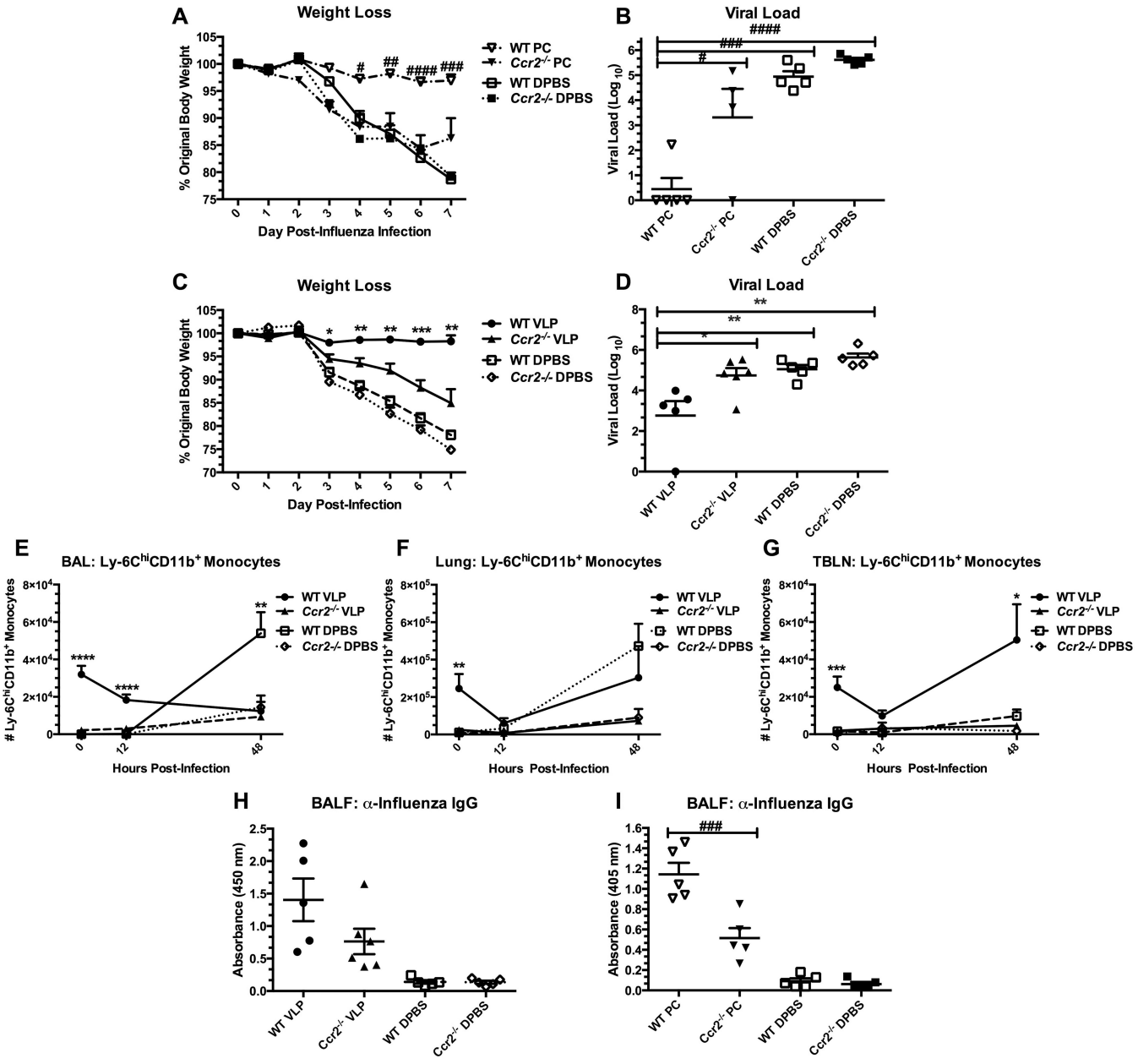

Figure 6.

Ccr2$^{-/-}$ mice are not protected from influenza virus via prior exposure to VLPs, or *Pneumocystis* infection. C57BL/6 (WT) or *Ccr2*$^{-/-}$ mice were infected with *Pneumocystis* (PC), or exposed to VLPs, or vehicle. Recovered mice were then challenged with 1.5×10^3 pfu PR8. Mice were weighed daily post-influenza infection (A&C), and viral load from the left lung lobe was determined at day 7 post-infection (B&D). In a second study of similar design (VLPs only), groups of mice were killed at 0, 12 hours, and 48 hours post-infection and the multilobe of the lungs and whole TBLNs were collected and prepared for FACS. Cells isolated from BAL (E), lung homogenate (F), and TBLN (G) were stained for Ly-6C$^+$CD11b$^+$ monocytes. Granulocytes were gated from forward and side scatter plots and resultant CD11c$^{lo/int}$ cells were gated and analyzed for their expression of Ly-6C and CD11b. For antibody determination, cell-free lavage fluid was analyzed by ELISA to determine the concentration of anti-influenza IgG (H&I). In figure 6H, BALF samples were

diluted 1:2 prior to analysis samples in figure 6I were plated neat. Data are shown as mean + SEM of n=5 from One-way ANOVA analysis with a Bonferroni's post-test. Significance as compared to the DPBS control group per strain is indicated by "#" for PC-infected mice and "*" for VLP-exposed mice. Experiments of similar design were independently performed at least twice.